15

On the Use of Wavelet Transform for Practical Condition Monitoring Issues

Simone Delvecchio
Engineering Department in Ferrara
Italy

1. Introduction

Condition monitoring is used for extracting information from the vibro-acoustic signature of a machine to detect faults or to define its state of health. A change in the vibration signature not only indicates a change in machine conditions but also points directly to the source of the signal alteration.

Fault diagnosis, condition monitoring and fault detection are different terms which are sometimes used improperly. Condition monitoring and fault detection refer to the evaluation of the state of a machine and the detection of an anomaly. Fault diagnosis could be set apart from other diagnoses since it is more rigorous and requires the type, size, location and time of the detected faults to be determined.

Due to their non-intrusive behaviour and use in diagnosing a wide range of mechanical faults, vibration monitoring techniques are commonly employed by machine manufacturers. Moreover, increases in computing power have helped the development and application of signal processing techniques.

Firstly, the monitoring procedure involves vibration signals to be acquired by means of accelerometers. Due to the selection of acquisition parameters being critical, the data acquisition step is not of minor importance. Sometimes, several steps, such as the correct separation of time histories, averaging and digital filtering is required in order to split the useful part of the signal from noise (electrical and mechanical), which is often present in industrial environments.

Secondly, signal processing techniques have to be implemented by taking into account the characteristics of the signal and the type of machine from which the signal is being measured (i.e. rotating or alternative machine with simple or complex mechanisms). In the final analysis, several features have to be extracted in order to assess the physical state of the machine or to detect any incipient defects and determine their causes.

When the nature of the signal varies over time, repeating the Fourier analysis for consequent time segments could describe the temporal variation of the signal spectrum. This well known technique is called Short Time Fourier Transform (STFT). The principal limitations of this approach are:

- only "average" results being obtained for each analysed time segment, requiring short analysis segments for good time resolution;
- the shorter the analysed time segment is, the coarser the resulting frequency resolution will be.

A more rigorous explanation of the latter is the Uncertainty Principle or Bandwidth-Time product that can be easily proved in [1] using the Parseval theorem and Schwartz inequality. This Principle states that:

$$\Delta f \cdot \Delta t \geq \frac{1}{4\pi} \tag{1}$$

where Δf is the frequency resolution expressed in Hertz and Δt is the time resolution expressed in seconds. It can be easily understood that Eq. 1 points to a limitation in STFT analysis methods: fine resolution in both time and frequency domains cannot be obtained at the same time.

Several techniques have been developed [2][3] to overcome this problem and to analyse different types of non-stationary signals.

As is reported in [2], one can distinguish between three important classes of non-stationary signals:

- Evolutionary Harmonic Signals related to a periodic phenomenon (i.e. rotation) of varying frequency;
- Evolutionary Broadband Signals with a broadband spectrum with spectral content evolving over time (i.e. road noise);
- Transient Signals which show a very short time segment of a wholly evolving nature (i.e. door-slam acoustic response and diesel engine irregularity within one combustion cycle).

Another important class of non-stationary signals is represented by Cyclostationary Signals which are not described here. Since this study deals with Transient signals, Wavelet Transforms (WT) have been proposed as an appropriate analysis tool.

In general, each type of fault produces a different vibration signature which might be detected by means of suitable signal processing techniques. Concerning i.c. engines, fault detection and diagnosis can be carried out using different strategies. One strategy can consist in modelling the whole mechanical system using lumped or finite element methods in order to simulate several faults and compare the results with the experimental data [4][5]. Another strategy is to adopt signal processing techniques in order to obtain features or maps that can be used to detect the presence of the defect [6][7]. Regarding the latter, a decision algorithm is require for a visual or automatic detection procedure. Moreover, maps can also be analysed for diagnostic purposes [8]. This method is used most commonly and is well suited to judgements involving expert technicians.

The latter strategy involves the application of time-frequency distribution techniques which are well suited for the analysis of non-stationary signals and have been widely applied to engine monitoring [9]-[11].

On the one hand, Short-Time Fourier Transforms (STFT), Wigner-Ville Distributions (WVD) and Continuous Wavelet Transforms (CWT) are usually used in order to distinguish faulty conditions for practical fault diagnosis and not to obtain reliable parameters for an automatic procedure led by a data acquisition system [9].

On the other hand, Discrete Wavelet Transforms (DWT) could be applied in order to extract informative features for an automatic pass/fail decision procedure [12]. Moreover, due to their power in identifying de-noising signals, the latter can be used in order to select frequency bands which are mostly characterised by impulsive components.

The aim of this study is to assess the effectiveness of both CWTs and DWTs for machine condition monitoring purposes. In this chapter, WTs are set up specifically for vibration signals captured from real life complex case studies which are poorly dealt with in literature: marine couplings and i.c. engines tested in cold conditions. Both Continuous (CWT) and Discrete Wavelet Transforms (DWT) are applied. The former was used for faulty event identification and impulse event characterization by analysing a three-dimensional representation of the CWT coefficients. The latter was applied for filtering and feature extraction purposes and for detecting impulsive events which were strongly masked by noise.

2. Background theory

This paragraph introduces the theory of fundamental background in order to understand achievements concerning the application of CWT and DWTs on real signals.

2.1 Continuous Wavelet Transforms

When referring to the definition of Fourier Transforms [1], it can be observed that this formulation describes the signal $x(t)$ by means of a set of functions $e^{j\omega t}$ which form the basis for signal expansions. These functions are continuous and of infinite duration. The spectrum in question corresponds to the expansion coefficients. An alternative approach consists of decomposing the data in time-localised waveforms. Such waveforms are usually referred to as wavelets. In recent decades, the theoretical background of wavelet transforms has been extensively reported ([14]-[19]).

The Continuous Wavelet Transform (CWT) of the time signal $x(t)$ is defined as:

$$CWT(a,b) = \frac{1}{\sqrt{a}} \int_{-\infty}^{+\infty} x(t)\psi^{*}\left(\frac{t-b}{a}\right)dt \tag{3}$$

with $a \in R^{+} - \{0\}, b \in R$.

This is a linear transformation which decomposes the original signal into its elementary functions $\psi_{a,b}$:

$$\psi_{a,b}(t) = \frac{1}{\sqrt{a}}\psi\left(\frac{t-b}{a}\right) \tag{4}$$

which are determined by the translation (parameter b) and the dilation (parameter a) of a so called "mother (analyzing) wavelet" $\psi(t)$.

The b translation parameter describes the time localization of the wavelet, while the a dilation determines the width or scale of the wavelet. It is worth noting that, by decreasing the a scale parameter, the oscillation frequency of the wavelet increases, but the duration of the oscillation also decreases, so it can be noted that exactly the same number of cycles is contained within each wavelet.

Therefore, an important difference when compared to the classical Fourier Analysis, in which the time window remains constant, is that the time and frequency resolution now becomes dependent on the a scale factor. For CWTs, in fact, the width of the window in the time domain is proportional to a, while the bandwidth in the frequency domain is proportional to $1/a$. Thus, in the frequency domain, WTs have good resolution for low frequencies and, in the time domain, good resolution for high frequencies; the latter property makes CWTs suitable for the detection of transient signals. More details and applications for CWTs can be found in literature ([20]-[24]).

Two kinds of mother wavelet are known in literature:

- the above defined mother wavelets which can be described by analytical functions;
- mother wavelets obtained by means of an iteration procedure, like orthogonal wavelets, which are well suited for performing Discrete Wavelet Transforms (DWT)[25].

Concerning the former, one of the most interesting is the Morlet wavelet which is defined as:

$$\psi(t)_{morlet} = \frac{1}{\pi^{-1/4}} e^{-t^2/2} e^{i2\pi f_0 t} \tag{5}$$

where f_0 is the central frequency of the mother wavelet. The term $1/\pi^{-1/4}$ is a normalization factor which ensures that the wavelet has unit energy; the Gaussian envelope $e^{-t^2/2}$ modulates the complex sinusoidal waveform. Since the Morlet wavelet is a complex mother wavelet, one can separate the phase and amplitude components within any signal when using it. The CWT result is graphically represented in the time-scale plane, while in this chapter the maps are displayed in the time-frequency domain, using the relationship $f = f_0 / a$ between the central frequency of the analyzing wavelet and the scale. Moreover, when complex analyzing wavelets are used, only the amplitude is considered and represented using a linear scale.

Concerning CWT implementation, the algorithm proposed by Wang and Mc Fadden was applied taking advantage of the FFT algorithm [26].

2.1.1 CWT improvements

Several improvements have been taken into account in this chapter in order to improve CWT power in detecting and localizing transients within a signal. These enhancements concern:

- the choice of mother wavelet;
- the time-frequency map representation;

- calculating the CWT of the TSA.

Firstly, as an initial improvement, the Impulse mother wavelet was taken into account in this work due to its capability in analysing impulses in vibration signals. It is defined as follows:

$$\psi(t)_{impulse} = \sqrt{2\pi} e^{2\pi i f_0 t - |2\pi t|} \cos(2\pi f_0 t) \tag{6}$$

where f_0 is the central frequency of the mother wavelets.

Its capabilities and the comparison between Morlet and Impulse mother wavelets in analysing transient signals are well reported in [27] and [28]. In this study, f_0 assumes the most common values found in literature: 0.8125 Hz for the Morlet mother wavelet and 20 Hz for the Impulse wavelet.

Secondly, a purification method inspired by the work of Yang [29] was considered in order to improve the accuracy of CWT representations and to try and solve the problem of frequency overlapping which has already reported in [10]. In [25] Yang applied the purification method using the Morlet wavelet, while in this paper the Impulse wavelet was also taken into account.

By means of purification methods, new CWT coefficients ($C\hat{W}T$) were calculated using the following equation:

$$C\hat{W}T(a,b,t) = \gamma(a,t) \cdot CWT(a,b,t) \tag{7}$$

The term $\gamma(a,t)$ is the coefficient of correlation between the original signal and the sinusoidal function with the frequency of the present wavelet scale given by ω_0 / a with ω_0 as the central frequency of the mother wavelet.

The correlation coefficient can be written as:

$$\gamma(a,t) = \left| \frac{\mathrm{cov}(x(T), H(a,T))}{\sigma_{f(T)} \sigma_{H(a,T)}} \right| \tag{8}$$

where $T \in [t - \tau/2; t + \tau/2]$, τ is the time duration of the signal *x(t)*, σ is the standard deviation, H is the sinusoidal function and a indicates the wavelet scale. The expression 'cov' means covariance and is defined for the two data histories x_1 and x_2 as:

$$Cov(x_1, x_2) = E\left[(x_1 - \mu_1)(x_2 - \mu_2)\right] \tag{9}$$

where E is the mathematical expectation and $\mu_1 = E[x_i]$.

It can be noted that the correlation between the signal and the sinusoid H is evaluated over a short time period defined by a time window with duration τ. In addition, the time window moves for the whole duration of the signal. After several tests, the choice of time window duration τ is based on a reliable compromise between the requirement of obtaining a higher correlation coefficient and the computational time needed for the correlation calculation.

In terms of the last CWT improvement, a new method which was recently proposed by Halim [30] was applied in order to compute the angular domain which averages across all the scales (TDAS) after CWT calculation. TDAS combines both wavelet analysis and the angular domain average in order to improve the time-frequency representation of the TSA of a signal. While the traditional method consists in taking wavelet transforms of the Time Synchronous Average, this new method performs the wavelet transformation first and then takes the time synchronous averages, obtaining the so-called TDAS distribution.

Assuming that the period of a time series is P and the time series has exactly M periods, the number of the total time samples is $N = P \cdot M$. If the number of wavelet scales s is S the wavelet transformation of the time series generates the complex matrix CWT (since both complex Morlet and Impulse mother wavelets have been applied) of $S \cdot N$ dimensions. It can be noted that each row of the absolute value of the CWT matrix is a time series corresponding to one s scale with a P period. If each of these time series is synchronously averaged (based on the period of the time series), the average of all the time series across all the scales can be computed obtaining the final TDAS matrix. Each row of the TDAS matrix represents the time synchronous average of the time series located at each scale. This method has the following advantages:

- it enables close frequencies to be detected due to the fact that the absolute value of the complex number is obtained after wavelet transformation has been obtained but before averaging. In fact, frequency detailed information could be lost if the wavelet transformation is computed after the averaging process;
- it permits higher noise reduction due to an improvement in the matching mechanism of the wavelet transform operator;
- it gives higher wavelet transformation resolution due to the higher number of samples processed since the transformation is computed over the entire time series.

On the basis of these considerations, this method appears to be helpful when a lower number of averages is available.

It is worth noting that Halim obtained the TDAS matrix using a geometric average and the Morlet wavelet as its basis. In this work, the effectiveness of the method using the Impulse mother wavelet is verified and the linear average is also taken into account in order to be consistent with the traditional method.

2.2 Discrete Wavelet Transforms

A Discrete Wavelet Transform (DWT) is a technique which enables discrete coefficients to be calculated by replacing the continuous coefficients obtained through CWT calculation [31]. Due to this fact, the a and b parameters in Eq. 2 become to the power-of-two:

$$a = 2^j, b = k2^j, j, k, \in Z \tag{10}$$

where j is called level, 2^j denoted the scale and $k2^j$ denotes the shift in the time direction.

The DWT is defined as:

$$c_{j,k} = \frac{1}{\sqrt{2^j}} \int_{-\infty}^{+\infty} x(t) \psi^* \left(2^{-j} t - k\right) dt \sum_{i=1}^{n} X_i Y_i \tag{11}$$

where the elementary function is

$$\psi_{j,k}(t) = 2^{-j/2} \psi\left(2^{-j} t - k\right) \tag{12}$$

and where $c_{j,k}$ are the wavelet coefficients or detail coefficients representing the time-frequency map of the original signal $x(t)$. This logarithmic scaling of both the dilation and translation steps is known as the dyadic grid arrangement.

The dyadic grid can be considered as the most efficient in discretization terms and leads to the construction of an orthonormal wavelet basis. In fact, discrete dyadic grid wavelets are commonly chosen to be orthonormal, i.e. orthogonal to each other and normalized to have unit energy. This means that the information stored in a $c_{j,k}$ wavelet coefficient is not repeated elsewhere and allows for the complete regeneration of the original signal without redundancy. Orthonormal dyadic discrete wavelets are associated with scaling functions $\phi_{j,k}(t)$. The scaling function has the same form as the wavelet, given by

$$\phi_{j,k}(t) = 2^{-j/2} \phi\left(2^{-j} t - k\right) \tag{13}$$

The scaling function is orthogonal to the translation of itself, but not to dilations of itself.

By means of the scaling function, it is possible to obtain the approximation coefficients $d_{j,k}$ with the same procedure as the wavelet function (i.e. convolving the scaling function with the signal):

$$d_{j,k} = \frac{1}{\sqrt{2^j}} \int_{-\infty}^{+\infty} x(t) \phi^* \left(2^{-j} t - k\right) dt \tag{14}$$

3. Condition monitoring of marine couplings

It is well known that diesel engines run very roughly at low speed ranges between 500-1000 rpm and that in marine applications they create vibrations in the body of the boat; moreover overall customer satisfaction with marine engines is based on performance in quietness terms.

Since speed limits (4 knots) are usually required to be respected on leaving ports, the duration of the departure is quite high; thus, it is necessary to maintain engine speeds at a minimum. Smooth running with very low vibration levels result from a dynamically balanced design with counterweights. Good torsional vibration analysis is required to enable low speeds without noise and vibration effects. Another typical vibration source at low speeds is diesel engine combustion pressure. If fuel is injected after a small delay, the rapid combustion causes a quick rise in the pressure with high-frequency excitation force components. An optimized injection system may eliminate fuel injection delay and the improved design of rigid cylinder blocks can reduce combustion pressure sources.

Finally, with regard to boat quietness, a general analysis is normally insufficient in evaluating the possibility of avoiding most noise and vibrations passing into the body of the boat through the crankshaft and the rigid coupling between the flywheel and the propeller shaft. It is necessary to highlight which parts are mainly related to vibration absorption. Coupling transmits torque and absorbs vibrations from the engine crankshaft. Placing a highly flexible coupling between the crankshaft and the propeller shaft will bring about further noise and vibration reduction. The vibration levels measured by the accelerometers mounted on different parts of the engine are a means of indicating which coupling works well.

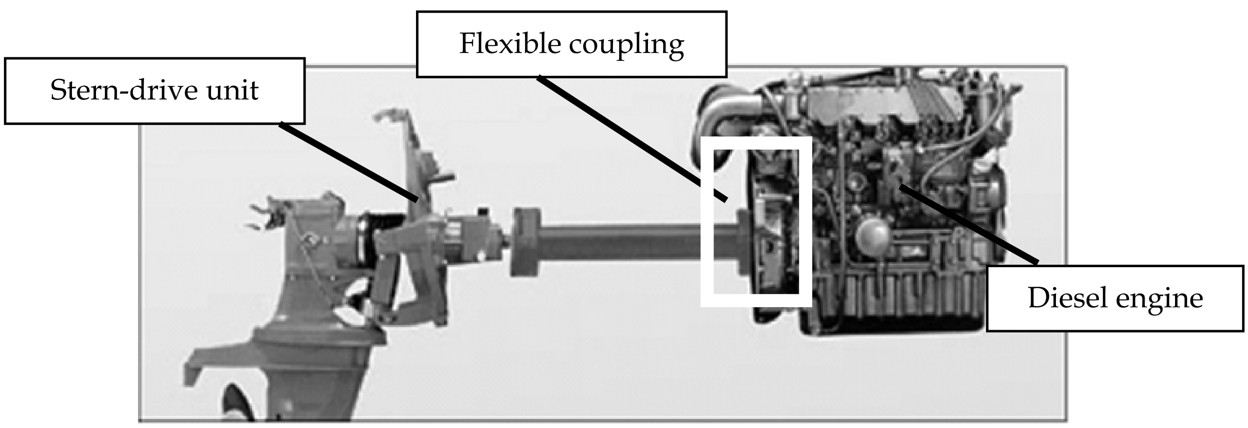

Fig. 1. Propulsion package with the flexible coupling under study.

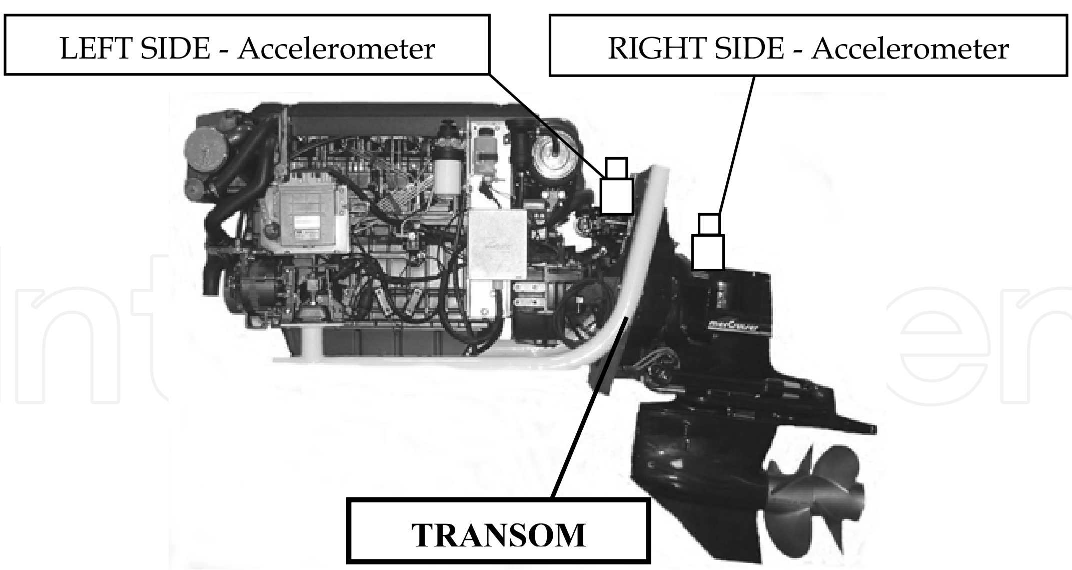

Fig. 2. Transom: position of accelerometers.

In the present study, Continuous (CWT) and Discrete Wavelet Transforms (DWT) are used to process the signals taken from a marine diesel engine in several operating conditions. The experimental results are presented and the capability of the above-mentioned analysis techniques are discussed.

One experimental investigation was carried out on a marine propulsion package (Fig. 1). The 4-cylinder 4-stroke diesel engine with eight valves was located inboard just forward of the transom. The engine was turbocharged with an exhaust-driven turbo-compressor: the turbo was controlled by a waste-gate valve.

Marine propulsion was assured by a stern-drive unit that contains the transmission and carries the propeller. The boat was steered by pivoting this unit with good characteristics in terms of speed, acceleration, steering and manoeuvring. In fact, the main advantage of stern-drives versus straight inboards is the possibility of changing the drive angle in order to obtain an optimum angle for speed or acceleration. The flexible coupling was mounted between the flywheel of the marine diesel engine and the propeller shaft. The primary side of the coupling was bolted to the flywheel, the secondary side was mounted onto the output shaft; between the two sides there were rubber elements which compensate for all types of misalignment, particularly angular, and dampen vibrations.

The vibration signals were measured from two points (see Fig. 2), which were close to the coupling, in order to analyse the vibration induced by the couplings at different angular positions of the stern drive when gears were repeatedly changed. The two accelerometers were mounted on both sides of the transom, that is, the left and right side. In order to compare the vibration behaviour of the two couplings, all compared vibration signals were picked up under exactly the same operating conditions.

Vibration signals were measured by means of piezoelectric tri-axial accelerometers (frequency range: 1-12000 Hz). All signal records were acquired starting from a crankshaft reference position: a tachometer signal was taken using an inductive proximity probe close to a gear wheel mounted onto the engine crankshaft.

In this context, DWTs were used to analyse the transom right-side signal in order to extract the scaling coefficients $d_{j,k}$. In fact, the signals in time domain obtained during tests, when the gears were repeatedly changed, revealed a train of impulsive components. Fig. 3 shows that the acceleration peaks are unclear in the signal measured from the transom right-side where the noise level was too heavy. In order to indicate which type of coupling provides better vibrational behaviour, the mean value of the acceleration peaks was obtained directly from the original time history from the transom left-side. Concerning the signal measured at the right side, the mean value was obtained for low frequency components at the first level $d_{1,k}$, after DWT application (Fig. 4) with the Symlet analysing wavelet.

Both types of couplings are very sensitive to transient dynamic phenomena due to gear changes. Table 1 shows that the mean value of the acceleration peaks for the Type 1 coupling is higher than the value for Type 2. Thus Type 2 gives better vibrational behaviour than the first type. It can be concluded that the time domain analysis of the coupling acceleration gives good condition monitoring information, if the DWT technique is used for signal denoising purposes.

In order to precisely localise the impulsive phenomena in the time-frequency domain and to validate the previous thesis about Type 2 vibrational behaviour, the Continuous Wavelet Transform for a frame of the transom left-side signal is applied. The impulse with the highest amplitude is isolated for this signal in the time domain, (Fig. 5) and the CWT of this part of the signal is calculated for the two different coupling types. In this work, a Morlet analysing wavelet was used, since its shape is similar to an impulse component.

Fig. 6 reports the wavelet analysis results revealing that the highest amplitude wavelet coefficients for Type 1 (Fig. 6(a)) are in the frequency range of around 1100 Hz. Regarding Type 2 (Fig. 6(b)), the wavelet transform amplitude during the transient phenomena assumes lower values and reveals an appreciatively constant amplitude in the 700-1500 Hz frequency range. The time-frequency plot is able to clearly show the frequency content during the impulse and gives a clearer interpretation of the difference vibrational behaviour of two coupling types.

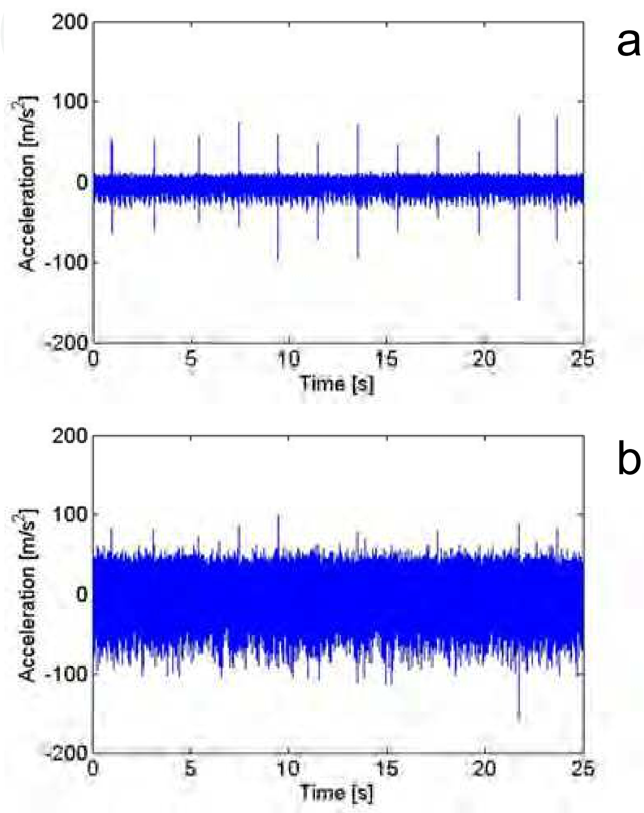

Fig. 3. The vibration signal (TYPE 2) from the transom left-side (a) and the transom right-side (b).

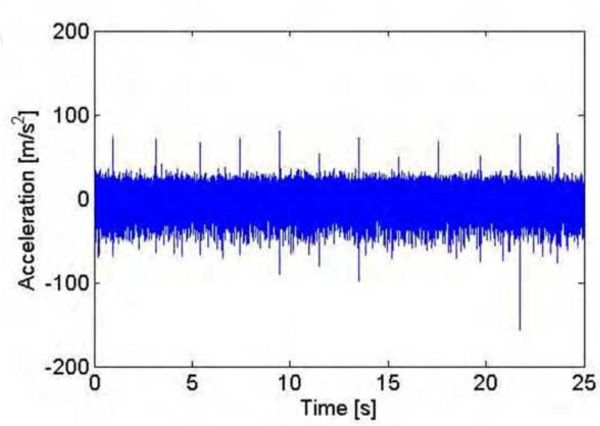

Fig. 4. DWT of the transom right-side signal (TYPE 2).

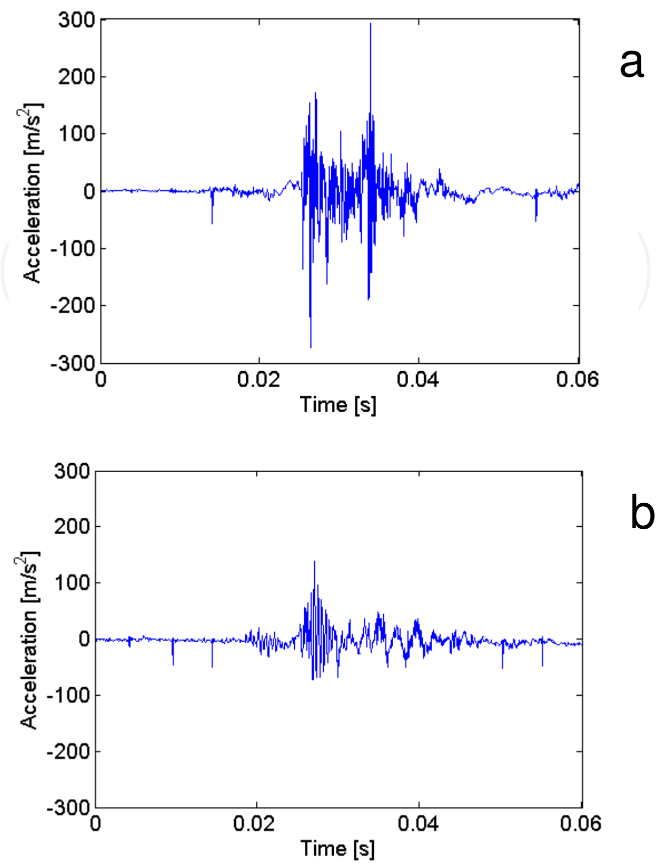

Fig. 5. Highest amplitude impulse for transom left-side acceleration. Coupling: Type 1 (a) and Type 2 (b).

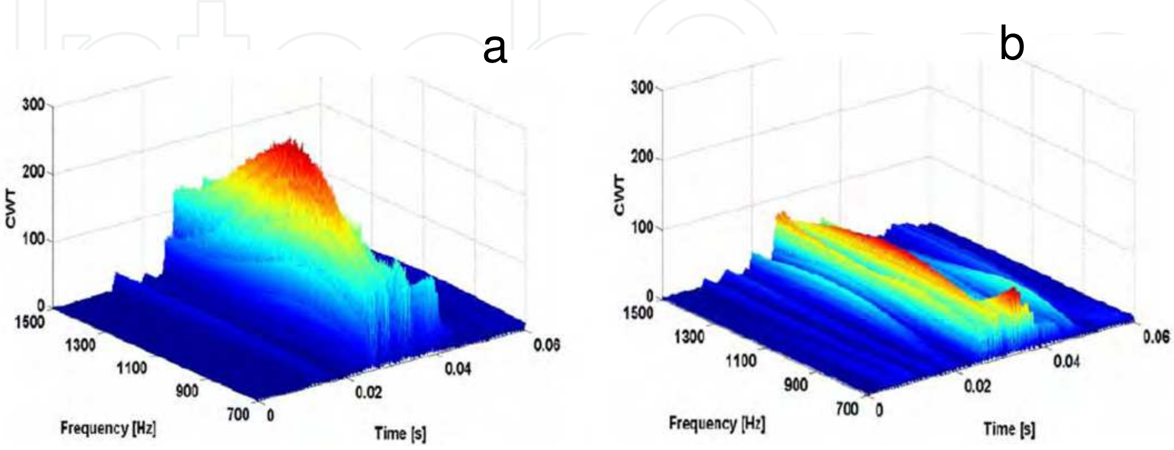

Fig. 6. Continuous wavelet transform (Morlet wavelet) for transom left-side acceleration, 700-1500 Hz frequency range; Coupling: Type 1 (a) and Type 2 (b).

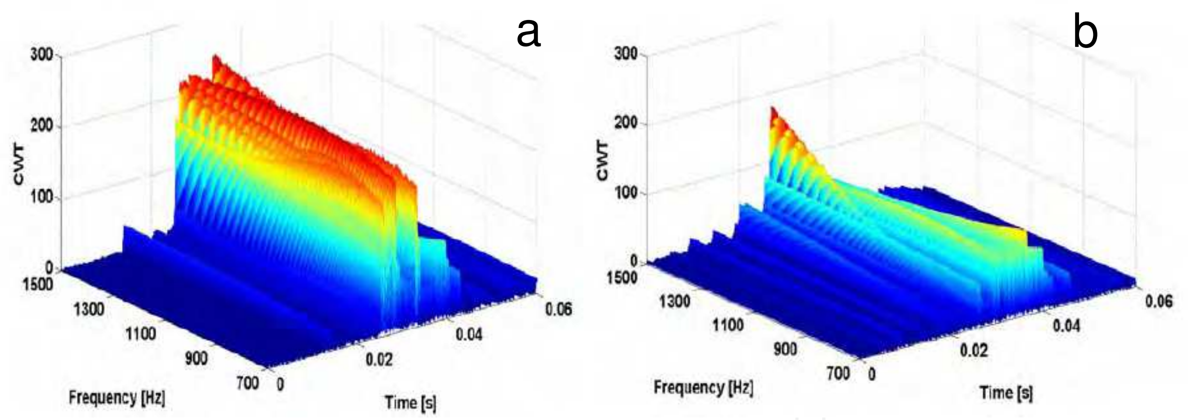

Fig. 7. Continuous wavelet transform (Mexican hat wavelet) for transom left-side acceleration, 700-1500 Hz frequency range; Coupling: Type 1 (a) and Type 2 (b).

Moreover, a comparison between two different Morlet and Mexican hat wavelet functions was evaluated. Undeniably, the Mexican hat wavelet function has a shape which is totally inadequate for analysing the signal impulse components. This is shown by the results in Fig. 7 which indicate that the Mexican hat highlighted the different frequency contempt of two coupling types but was not able to precisely localise the higher frequency components of the impulse signal.

4. Condition monitoring of I.C. engines in cold conditions

This second application addresses the use of CWT and DWTs as a means of quality control for assembly faults in diesel engines using cold test technology. Nowadays, the majority of engine manufacturers test their engines by means of "hot tests", i.e. tests in which the engine is firing. Hot tests are mainly aimed at determining engine performance.

Recently, some companies have introduced "cold tests" which aim to identify assembly anomalies by means of torque, pressure and vibration measurements. Cold tests are more oriented towards identifying the source of anomalies since they are not affected by noise and vibration due to firing. Reciprocating machines, such as IC engines, give non-stationary vibration signals due to changes in pressure and inertial forces and valve operations. Therefore, WTs are an efficient tool for analyzing transient events during the entire engine operation cycle.

Here, CWTs are applied in order to obtain an accurate fault event identification for signals measured from engines with different assembly faults that have not been considered in literature. The analysis takes advantage of cyclostationary modelling developed and tested by Antoni in [8].

Experimental investigations were carried out on a 2.8 dm^3 4-cylinder 4-stroke, four-valve-per-cylinder turbocharged diesel engine with an exhaust-driven turbo-compressor produced by VM Motori. The measurements were carried out in cold conditions (without combustion) while the engine crankshaft was driven by an electric motor via a coupling. The acceleration signal was measured by means of a piezoelectric general purpose accelerometer mounted on the engine block (turbocharger side) close to the bearing support of the crankshaft. A 360 pulse/rev tachometer signal was used to measure the angular position of the crankshaft. During acquisition, the acceleration signal was resampled with a 1 degree angular resolution.

The first faulty condition concerned an engine with a connecting rod with incorrectly tightened screws, that is, screws which were only tightened with a preload of 3 kgm, instead of the correct torque of 9. The second faulty condition concerned an engine with an inverted piston, with incorrectly positioned valve sites. This incorrect assembly hindered the correct correspondence between the valve plates and the valve sites. Since the exhaust valve site area is larger than the intake valve site, the exhaust valves knocked against the non-correspondent intake valve sites.

Fig. 8(a) shows that the CWT map (Impulse wavelet) of the Time Synchronous Average (TSA) detected four cylinder pressurizations and two events related to the faulty condition. Even if a remarkable vertical line at 100 degrees was present in the CWT map of the TSA (Fig. 8 (a)), it is not sufficient to assure the presence of a mechanical fault since its amplitude is comparable to the pressurization peak amplitudes. Therefore, the CWT of the residual signal (i.e. the signal obtained by subtracting the time synchronous average from the raw signal) is an expected step in mechanical fault localization within engine kinematics (Fig. 8(b)). As depicted in Fig. 8(b), the presence of the pre-loaded rod is highlighted by a marked vertical line at about 100º.

As explained in [32] the peak is caused by the absence of controlled bush deformation when the correct tightening torque is not applied. This clearance is abruptly traversed whenever a change in the direction of the resultant force occurs on the rod. In particular, it was demonstrated that the acceleration peak took place at the beginning of the cylinder 3 intake stroke, corresponding to cylinder 2 pressurization (i.e. 'Press 2' in Fig. 8(a)). Hence, fault location can be only achieved by the analysis of the residual signal. It is worth noting that better angular fault localization can be achieved using the Morlet mother wavelet (Fig. 8(c)) which gives lower frequency resolution but higher angular localization of the angle-frequency map. Since the purpose of the proposed approach is to obtain reliable fault diagnostics through accurate angular transient event localization, the Morlet wavelet can be considered the most desirable if compared with the Impulse wavelet.

In order to improve the CWT of the TSA, the purification method was firstly carried out using correlation weighted CWT coefficients, i.e. $\hat{CWT}$, as described in Section 2.1.1.

As previously mentioned, the correlation coefficient $\gamma(a,t)$ used in this method is able to select which coefficient gives the best match between the frequency of the signal and the frequency corresponding to the Impulse wavelet scale.

Fig. 9(a) shows that this method provides a clearer representation in terms of sensitivity to background noise. However, the use of the coefficient correlation method does not improve the angular localization of the main engine events. As noted earlier, this enhancement can be obtained using the Morlet mother wavelet. The Morlet mother wavelet was used to compute the wavelet transform by means of both traditional and TDAS methods. No significant improvements in angular faulty localization can be obtained by using the TDAS method (Fig. 9(b)). Therefore, it can be concluded that a traditional CWT map with a Morlet mother wavelet is sufficient for faulty localization purposes.

It should be noted that CWT is used in order to distinguish faulty conditions from normal ones for practical fault diagnosis and not to obtain reliable parameters for an automatic procedure led by a data acquisition system.

In order to overcome this issue, the DWT technique for the extraction of faulty components from the signal, proposed by Shibata, was evaluated for the second fault which was condition tested, i.e. the inverted piston.

Fig. 10 shows the DWT coefficients ($c_{j,k}$) when Symlet (eight order) is used for the wavelet and the scaling function. Data sampled at 70 μs were used for the DWT.

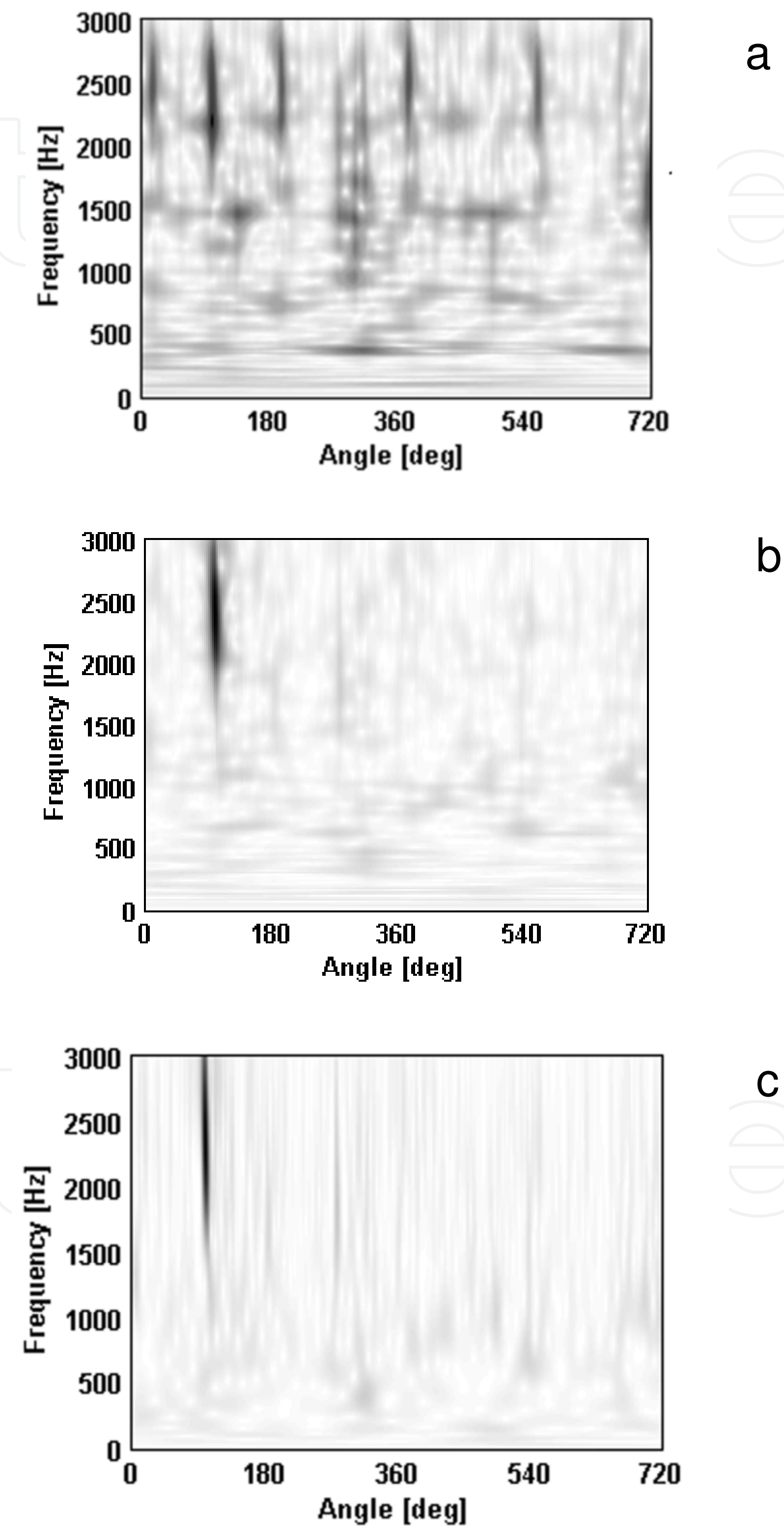

Fig. 8. Faulty engine – (a) CWT (impulse wavelet) of the TSA, (b) residual signal (impulse wavelet); (c) CWT (morlet wavelet) of the residual signal.

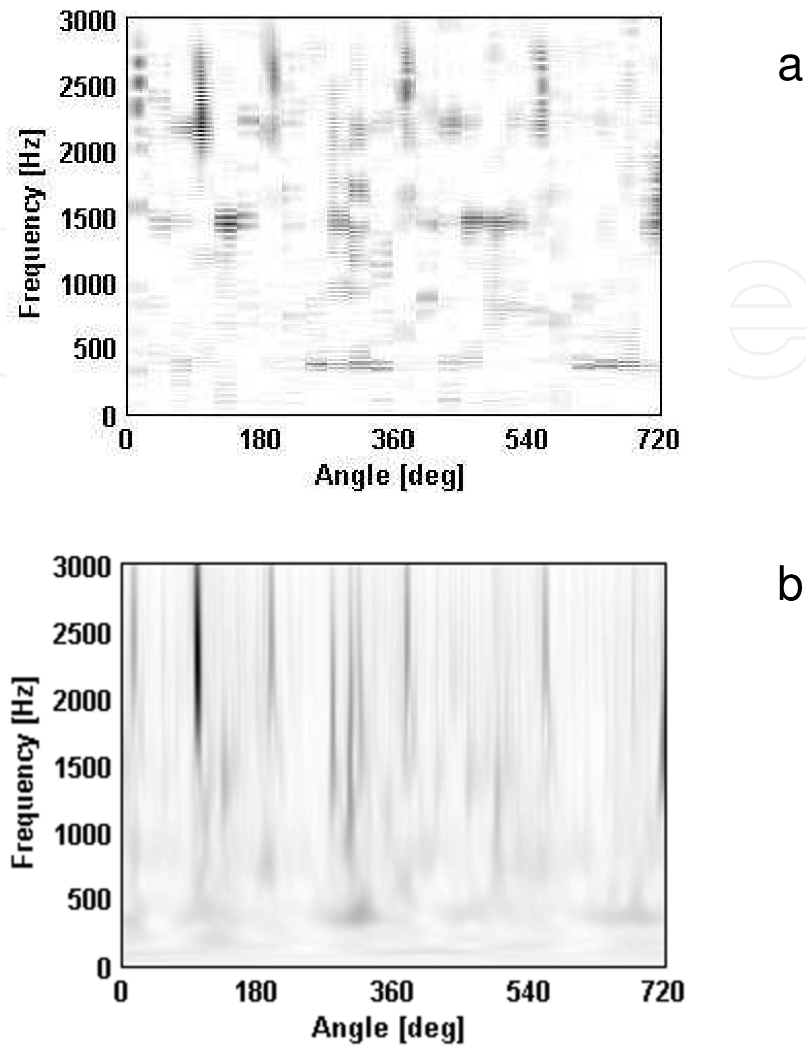

Fig. 9. Faulty engine – (a) CWT of the TSA: purification method (impulse mother wavelet); (b) TDAS method (morlet mother wavelet).

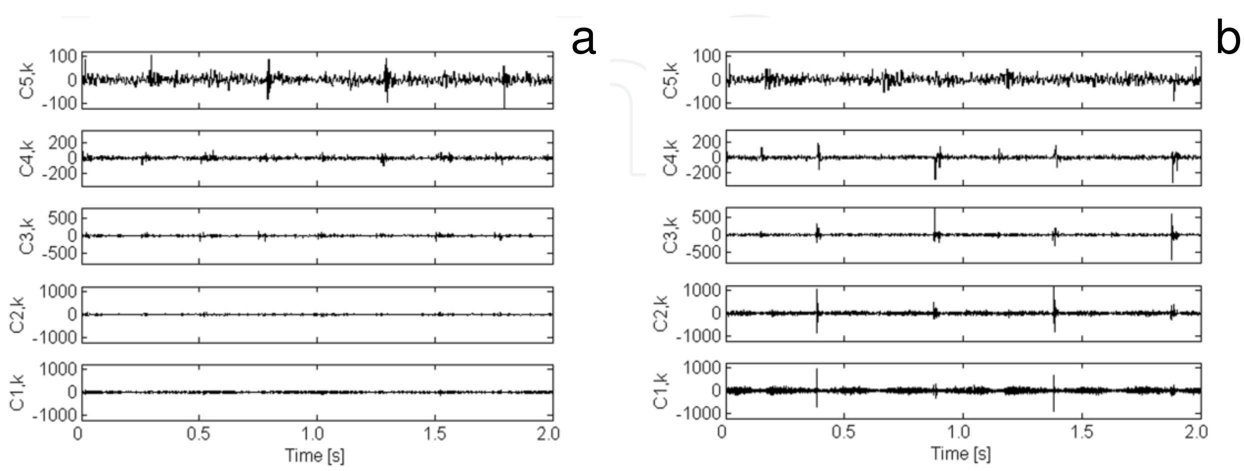

Fig. 10. DWT coefficients for the vibration signals (120 rpm): (a) Normal condition; faulty condition (piston inverted).

Coupling	Original transom left side signal	DWT of the transom right side signal
TYPE 1	102.25	121.13
TYPE 2	58.61	72.87

Table 1. Mean value of the peaks of acceleration (m/s^2).

Level $C_{j,k}$	Ratio of RMS F/N Inverted piston
-	1.11
j = 5	1.01
j = 4	1.60
j = 3	2.26
j = 2	3.50
j = 1	**3.76**

Table 2. Comparison with coefficients of DWT: ratio of RMS value between the faulty (F) and normal (N) conditions.

Table 2 shows the comparison between the RMS ratio of the DWT coefficients in faulty (F) and normal (N) conditions with the engine running at 120 rpm. The j = 1 level shows the highest difference between the faulty and normal vibration signals. Thus, the RMS ratio at the first decomposition level may be considered a reliable monitoring feature.

5. Conclusions

This chapter deals with WT applications for practical condition monitoring issues on flexible couplings and i.c. engine. In particular, CWT and DWT capability was assessed. The former was used for faulty event identification and impulse event characterization through the analysis of three-dimensional representations of CWT coefficients. The latter was applied for filtering and feature extraction purposes and for detecting impulsive events which were strongly masked by noise. Several CWT representation improvements were also evaluated.

Comparing the results from both the CWT and DWT analyses, the ability of WTs in satisfying both condition monitoring and fault detection requirements for all tested cases was clearly demonstrated. In particular, traditional CWTs of the residual signal (i.e. the signal obtained by subtracting the time synchronous average from the raw signal) with the Morlet mother wavelet was revealed to be the most powerful tool in angularly localizing the assembly fault within the engine kinematics.

It can be concluded that the application of WTs not only enables changes in the state of the tested machine to be recognized but also the localisation of the source of the alteration.

6. Acknowledgments

This work was developed within the Advanced Mechanics Laboratory (MechLav) of Ferrara Technopole and brought into being with a contribution by the Emilia-Romagna Region – Assessorato Attivita' Produttive, Sviluppo Economico, Piano telematico - POR-FESR 2007-2013, Attività I.1.1.

7. References

[1] Papoulis, A., 1962, The Fourier Integral and its applications. McGraw-Hill, New York.

[2] Van der Auweraer, H., et al., (1992), Spectral estimation of time-variant signal, in *Proceedings of ISMA17 International Conference on Noise and Vibration Engineering*, Leuven, Belgium, pp. 207-223.

[3] Van der Auweraer, H., et al., (1992), Analysis of non-stationary noise and vibration signals, in Proceedings of ISMA17 International Conference on Noise and Vibration Engineering, Leuven, Belgium, pp. 385-405.

[4] Bartelmus, W., (2001), Mathematical modelling and computer simulations as an aid to gearbox diagnostics, *Mechanical Systems and Signal Processing*, 15, 855-871.

[5] Jid, S., Howard, I., (2006) Comparison of localized spalling and crack damage from dynamic modelling of spur gears vibrations, *Mechanical Systems and Signal Processing*, 20332-349.

[6] Wu, J.D. and Chuang, C.Q. ,(2005). "Fault diagnosis of internal combustion engines using visual dot patterns of acoustic and vibration signals", *NDT&E International*, 38(2005), pp. 605-614.

[7] Shibata, K., Takahashi, A., and Shirai, T. (2000). Fault diagnosis of rotating machinery through visualisation of sound signal, *Mechanical Systems and Signal Processing*, 14, 229-241.

[8] Antoni, J., Daniere, J., and Guillet, G. (2002), Effective vibration analysis of ic engines using cyclostationarity. Part I-A methodology for condition monitoring, *Journal of Sound and Vibration*, 257, 815-837.

[9] Da Wu, J., Chen Chen, J. (2006), Continuous wavelet transform technique for fault signal diagnosis of internal combustion engines, *NDT&E International*, 39, 304-311.

[10] Tse, P., Yang W., Tam, H. Y., (2004), Machine fault diagnosis through an effective exact wavelet analysis,, *Mechanical Systems and Signal Processing*, 277, 1005-10024.

[11] Geng, Chen, J., Barry Hull, J. ,(2003). Analysis of engine vibration and design of an applicable diagnosing approach, *International Journal of Mechanical Sciences*, 45, 1391-1410.

[12] Farag K. Omar, A.M. Gaouda (2012), Dynamic wavelet-based tool for gearbox diagnosis, *Mechanical Systems and Signal Processing*, 26, 190-204.

[13] Loutas, T. H., Roulias, D., Pauly, E., Kostopoulos, V. (2010). The combined use of vibration, acoustic emission and oil debris on-line monitoring towards a more effective condition monitoring of rotating machinery, *Mechanical Systems and Signal Processing*, 25, 1339-1352.

[14] Torrence, C., (1998), A Pratical Guide to Wavelet Analysis. Bulletin of the American Meteorological Society, 79(1).

[15] Peng, Z.,K., Chu, F. L., (2004), Application of the wavelet transform in machine condition monitoring and fault diagnostics: a review with bibliography, *Mechanical Systems and Signal Processing* 18, 199-221.

[16] Al-Badour, F., Sunar, M., Cheded, L. (2011), Vibration analysis of rotating machinery using time–frequency analysis and wavelet techniques, *Mechanical Systems and Signal Processing*, 25, 2083-2101.

[17] Newland, E., 1994, Wavelet Analysis, Part I: Theory, *Journal of Sound and Vibration* 116, 409-416.

[18] Newland, E., 1994, Wavelet Analysis, Part II: Wavelet Maps, *Journal of Sound and Vibration* 116, 417-425.
[19] Mallat, S., A wavelet tour of signal processing. Academic Press, 1999.
[20] Lin, J., Zuo, M., J., (2003), Gearbox fault diagnosis using adaptive wavelet filter, *Mechanical Systems and Signal Processing* 17(6), 1259-1269.
[21] Boulahbal, D., Golnaraghi M., F., Ismail, F., (1999), Amplitude and phase wavelet maps for the detection of cracks in geared systems, *Mechanical Systems and Signal Processing* 13(3), 423-436.
[22] Baydar, N., Ball, A., (2003), Detection of gear failures via vibration and acoustic signals using wavelet transform, *Mechanical Systems and Signal Processing* 17(4), 787-804.
[23] Meltzer, G., Dien, N., P., (2004), Fault diagnosis in gears operating under non-stationary rotational speed using polar wavelet amplitude maps, *Mechanical Systems and Signal Processing* 18, 985-992.
[24] Wang, W., J., (1995), Application of orthogonal wavelets to early gear damage detection, *Mechanical Systems and Signal Processing* 9(5), 497-507.
[25] Berri, S., Klosner, J., M., (1999), A new strategy for detecting gear faults using denoising with the orthogonal Discrete Wavelet Transform (ODWT), in *Proceedings of the 1999 ASME Design Engineering Technical Conferences*, September 12-15, 1999, Las Vegas, Nevada.
[26] Wang, W. J., McFadden, P. D., (1996), Application of wavelets to gearbox vibration signals for fault detection, *Journal of Sound and Vibration*, 192, 927–939, 1996.
[27] D' Elia, G., 2008, Ph.D. Thesis in Applied Machines, Fault detection in rotating machines by vibration signal processing techniques, Universita' di Bologna, Italy.
[28] Schukin, E.L., Zamaraev, R.U., Schukin, L.I., (2004), The optimization of wavelet transform for the impulse analysis in vibration signals. *Mechanical Systems and Signal Processing*, 18, 1315-1333.
[29] Yang, W., (2007), A natural way for improving the accuracy of the continuous wavelet transform. *Journal of Sound and Vibration*, 306, 928-939.
[30] Halim B. et al., (2008), Time domain averaging across all scales: A novel method for detection of gearbox faults, *Mechanical Systems and Signal Processing*, 22, pp. 261-278.
[31] Addison P. S., (2002), The Illustrated Wavelet Transform Handbook, Istitute of Physics Publishing, Philadelphia.
[32] Delvecchio, S., D'Elia, G., Mucchi, E. and Dalpiaz, G. (2010). Advanced Signal Processing Tools for the Vibratory Surveillance of Assembly Faults in Diesel Engine Cold Tests. *ASME Journal of Vibration and Acoustics*, Volume 132, Issue 2, 021008 (10 pages).

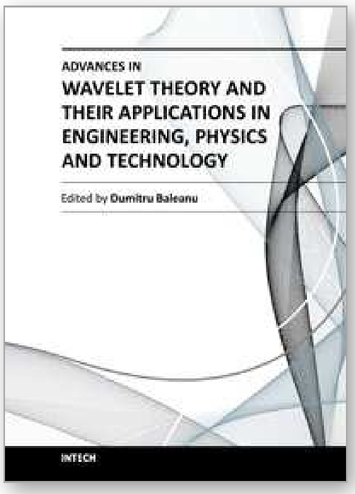

Advances in Wavelet Theory and Their Applications in Engineering, Physics and Technology
Edited by Dr. Dumitru Baleanu

ISBN 978-953-51-0494-0
Hard cover, 634 pages
Publisher InTech
Published online 04, April, 2012
Published in print edition April, 2012

The use of the wavelet transform to analyze the behaviour of the complex systems from various fields started to be widely recognized and applied successfully during the last few decades. In this book some advances in wavelet theory and their applications in engineering, physics and technology are presented. The applications were carefully selected and grouped in five main sections - Signal Processing, Electrical Systems, Fault Diagnosis and Monitoring, Image Processing and Applications in Engineering. One of the key features of this book is that the wavelet concepts have been described from a point of view that is familiar to researchers from various branches of science and engineering. The content of the book is accessible to a large number of readers.

InTech Europe
University Campus STeP Ri
Slavka Krautzeka 83/A
51000 Rijeka, Croatia
Phone: +385 (51) 770 447
Fax: +385 (51) 686 166
www.intechopen.com

InTech China
Unit 405, Office Block, Hotel Equatorial Shanghai
No.65, Yan An Road (West), Shanghai, 200040, China
中国上海市延安西路65号上海国际贵都大饭店办公楼405单元
Phone: +86-21-62489820
Fax: +86-21-62489821